# Design of Koch Curve-Based Fractal Antenna for Ultra-Wideband Applications

Khushbu Patel
*Dept. of Electronics and Communication Engineering*
*National Institute of Technology*
Rourkela, India
khushbupatel869@gmail.com

Santanu Kumar Behera
*Dept. of Electronics and Communication Engineering*
*National Institute of Technology*
Rourkela, India
skbehera@ieee.org

*Abstract*— **This article proposes a new fractal antenna design for Ultra-Wideband (UWB) applications. The final design topology is attained by a Koch curve fractal-based pentagonal radiator, the partial ground, and a microstrip feedline, to realize a novel fractal antenna with a small footprint, better structural conformability, and wide Impedance Bandwidth (IBW) to operate in the UWB. The band of the antenna design functions at the 3 GHz to 12 GHz band. A 2$^{nd}$ order Koch curve fractal is employed along the inner edges of the radiator. The proposed antenna is designed using HFSS 2020 software and also printed on a substrate Roger RT/Duroid 5880 having a dielectric constant ($\varepsilon_r$ = 2.2). It shows a peak realized gain of 4.7 dBi at 4.1 GHz covering the operating band. The miniaturized dimension of the proposed design (30 × 30 × 1 mm$^3$), acceptable values of gain, efficiency, Cross-Polar discrimination (XPD) of 40 dB, and low profile, make the linearly polarized fractal antenna suitable for UWB applications.**

***Keywords*-Koch fractal, ultra-wideband, Roger RT/Duroid substrate, bandwidth, partial ground.**

## I. Introduction

Antennas can be designed in two ways. The primary is numerous antennas, where each antenna uses a different frequency. A single antenna that covers numerous frequency bands is the second option. The second option is better and more suitable for their needs as modern devices are generally portable. Multiband radiating devices and technologies for advanced communication services have attracted the attention of researchers as these devices meet the requirements of telecommunication devices operating on multifrequency ranges with specific wireless devices. Several wireless networks are supported by antennas with several operating bands. Recent devices for communication are portable, thus the required antenna requires to be small, have a wide IBW, and have excellent radiation features like high efficiency and gain [1-3]. Antenna performance properties are improved using a fractal structure. Fractal antennas significantly enhance the performance of radiation patterns designed for many different kinds of applications across a range of frequencies in the context of devices that are capable of capturing and radiating a range of waves in connection with Electromagnetic (EM) signals. Recently, many fractal geometries have been used in antennas to improve antenna properties by increasing the degree of freedom [4]. A fractal-based antenna design is another structure utilized by researchers to address dimension limitations. The design of the patch may be various shapes, such as square [5], star [6], Pythagorean-tree-shaped fractal [7], Sierpinski gasket fractal [8], Peano-Gosper fractal [9], Koch fractal [10], [11], Minkowski Island curve and Koch curve fractals [12], Hilbert [13], and Vicsekcross-shaped fractal [14]. The radiator miniaturization approaches utilizing fractal structure and features of the fractal method such as self-similarity and gap filling are helpful to obtain a wide band. The electrical dimension is increased via gap filling, and a wide bandwidth is produced by self-similarity. For the first time, the fractal dimension of the structure has been connected to a fractal antenna design utilizing Koch curves for various resonant frequencies. Werner and Ganguly offer a thorough analysis of fractal antenna engineering research [4]-[7]. While specific fractal geometries can be employed for multiband/wideband wireless services, certain fractal designs can be used to reduce the antenna's size. A fractal structure can be produced over the span of multiple iterations with the use of a Multiple Reduction Copy Machine (MRCM) algorithm. Koch curve fractal structure is a standard structure in the category of fractal-based designs. [8]-[10]. The majority of fractal objects have self-similar shapes and sizes. MRCM technique can be employed to execute an infinite number of iterations to create the fractal shape. An antenna element's electrical length increases when the space-filling property is used [11], [12].

A popular microstrip antenna that is extensively researched in Partial Discharge Monitoring (PDM) is the Hilbert fractal antenna. The article presents a 4$^{th}$-order Hilbert fractal-based radiating element for partial discharge detection in oil-paper insulated devices [13]. In [14], a circularly polarized design structure utilizing a fractal-based slot design is explored for use in Radio Frequency Identification (RFID) handheld readers. The antenna comprises a coaxial feed positioned 45$^0$ away from the slot and a vicsekcross-structured slot carved along a diagonal axis to produce circular polarization. Further, the article [15] investigates the use of both fractal structure and EM bandgap realizations in the antenna and the execution of the UWB antenna for wireless devices in the satellite communication bands. Furthermore, a triple band antenna with a small footprint, lightweight, and inexpensive price is designed for wireless applications. The Koch curve-based technique was proposed in the study for creating a triple-band microstrip radiator [16]. Antenna performance shows that the microstrip radiating element functions in three bands when the Koch fractal structure is used. Recent years have seen the suggestion and investigation of a large number of UWB antenna layouts based on fractal structures, including Sierpinski, Minkowski, Koch, Cantor, and Hilbert fractal designs. Though there are many advantages to Prevailing fractal geometries, some of them have limitations, such as wideband performance for a small frequency range [17], [18].

The aim of this article is to design a miniaturized antenna that has various operational frequency bands that is capable of covering the required frequency range for RFID, Global Positioning System (GPS), LTE, 3G, WiMax, Wi-Fi, Industrial Scientific, Medical (ISM), and satellite applications while providing suitable gain and efficiency. The proposed work presents a fractal antenna using Koch curve geometry with the help of ANSYS HFSS 2020 software. A partial ground technique with a rectangular-shaped slit is applied on the ground to obtain a wideband. The designed radiator has an operational IBW of 9 GHz from 3 GHz to 12 GHz for UWB applications. The article is arranged in the given sections. Section 2 offerings an overview of the fundamentals of fractal antenna topology and design structure. This part shows details of the design technique of creating a Koch curve-based fractal and the evolution of the proposed design with dimensional parameters. In section 3, the performance study of the design is described. Section 4 focuses on the performance comparison of the designed antenna to the existing work. The conclusions are summarized in section 5.

## II. FRACTAL ANTENNA TOPOLOGY AND DESIGN

### A. Koch fractal geometry

A fractal antenna uses a fractal, self-similar design to maximize the effective length or increase the perimeter of a radiating element to enhance the antenna performance. Fig. 1 displays the fractal structure of the Koch curve. It is a line segment taking parts signified as $\beta$. The segment of the part is split into a group of three sub-parts, denoted as $\beta/3$. The length of the separated segments of $\beta_1$, $\beta_2$, and $\beta_3$ is $L/3$. Iteration is the term used to describe this continuous repetition of portion division.

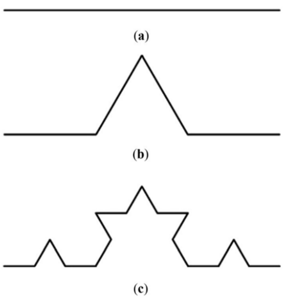


Fig. 1. Koch curve iterations: (a) 0th order, (b) 1st order, and (c) 2nd order [1].

The segment is split by a factor of 3 for each iteration of the line $L$, starting with $L_1 = L/3$, continuing with $L_2 = L/9$ for the 2nd iteration, $L_3 = L/27$ for the 3rd, and so on until the $n^{th}$ iteration. The equations that apply for Koch curve-based structure and iterations to the $n^{th}$ order are (1), (2), and (3). Equation (4) demonstrates that the Koch curve is $(4/3)^n$ for the entire length of the line segment $L$. Higher-order iterations of the fractal structure were not feasible due to the limitations and fabrication difficulties. Thus, the 2nd iteration has been considered the most appropriate iteration of the design in this research endeavor.

$$\beta_1 = L/3 \rightarrow L_1 = 4\beta \quad (1)$$

$$\beta_2 = L/3 \rightarrow L_2 = 16\beta \quad (2)$$

$$\beta_n = L/3 \rightarrow L_n = 4^n\beta_n \quad (3)$$

$$L = (4/3)^n \quad (4)$$

### B. Fractal Antenna Design Flow

Fractal geometry embedded in a patch design has a direct effect on the operating band. In the initial stage, the antenna geometry is modeled as a regular pentagonal patch in antenna 1, and in the next stage, the pentagonal-structured slot is etched from the middle portion of the patch (antenna 2). Further, in the antenna structure, a 2nd iteration of the Koch curve-based fractal is executed along the inner part of the patch element. Fig. 2(b–d) demonstrates the iteration of the Koch curve fractal structure. 0th, 1st, and 2nd order of iterations of the Koch curve fractal structure are depicted in Fig. 5. It is noticed that, as the number of iterations increases, the operating frequency band of the radiator becomes increased with a broad frequency range covering 3 GHz to 12 GHz.

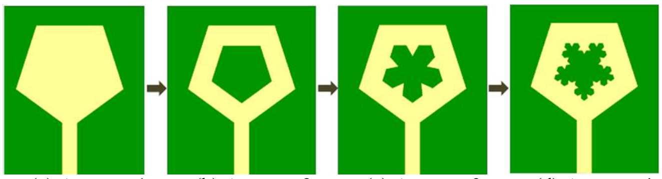

(a) Antenna 1 (b) Antenna 2 (c) Antenna 3 (d) Antenna 4

Fig. 2. Evolution of proposed design.

### C. Fractal Design Layout

The final dimensions of the fractal antenna are provided in Table I, and its geometry is displayed in Fig. 3. Koch curve fractal is employed to the inner part of the pentagonal ring patch up to the 2nd order of iteration. The antenna design dimensions are also specified in Fig. 3. The objective of utilizing such a shape is to increase space-filling, which results in reduced antenna physical dimension as well as increased resonant frequency bands. The microstrip line of 50 Ω is used to feed the antenna through a matching part over the ground plane. The patch is employed on the Roger RT/Duroid 5880 substrate having the dimension of 30 × 30 × 1 $mm^3$. The patch is positioned on one side of the substrate and the partial ground plane is located on the other side. The overall dimensional parameters of the RFA are given in Table I.

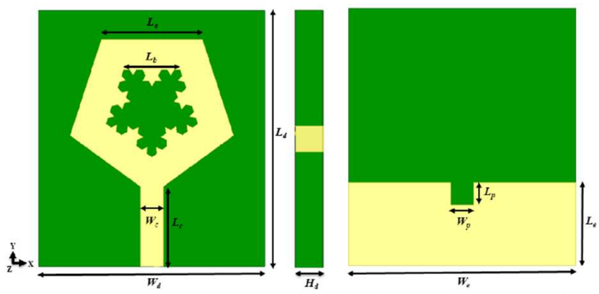

(a) Front view (b) Side view (c) Rear view

Fig. 3. Schematic diagram of reconfigurable fractal antenna.

TABLE I. Design Specifications

| Parameters | Notations | Values (mm) |
|---|---|---|
| Side of radiating element | $L_a$, $L_b$ | 12, 7 |
| Length of feed line | $L_c$ | 12 |
| Width of feed line | $W_c$ | 3 |
| Length of ground | $L_e$ | 12 |
| Width of ground | $W_e$ | 30 |
| Rectangular slit length | $L_p$ | 3 |
| Rectangular slit width | $W_p$ | 3.5 |

## III. Discussion of Antenna Performance

This section provides a thorough overview of linearly polarized antenna performance parameters in terms of $S_{11}$, gain, radiation beams, and current distribution. The IBW of a radiating element denotes the overall frequency range in which the radiator can work suitably.

### *A. Surface Current Analysis*

The surface current distribution plots are obtained at 6.2 GHz for all antenna iterations in Fig. 2. As can be realized collectively in Fig. 2(a)-(d), the wide-band features are caused by surface currents along the Koch fractal-based structure with pentagonal patch sides, where they acquire additional resonances. These resonances produce enhanced gain related to the extended electrical length of the fractal radiating element. The fractal characteristics of the radiator enable miniaturization of the radiator design and ensure wide-band performance due to the concentration of current on the inner and outer edges. The wider IBW is due to the accumulated charge at the Koch curve fractal boundaries and along the inner and outer boundaries of pentagons, which validates the radiator's wide-band performance owing to the electrical length of the fractal geometry. The current distribution plots make it clear that the radiator's center and lower parts are where the current is concentrated the most.

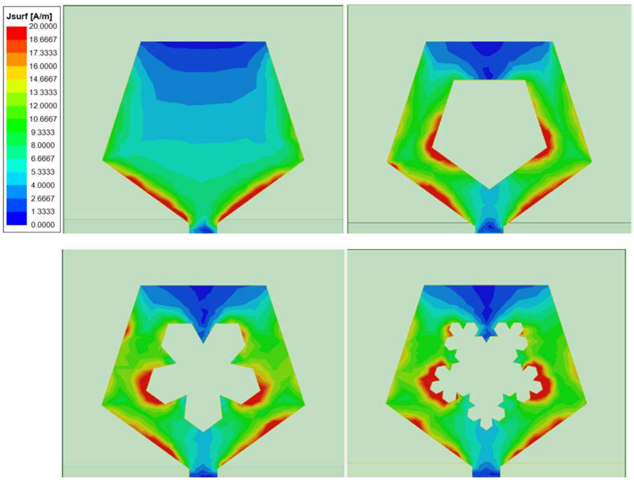


Fig. 4. The current distribution plots at 6.2 GHz (a) antenna 1, (b) antenna 2, (c) antenna 3, and (d) antenna 4.

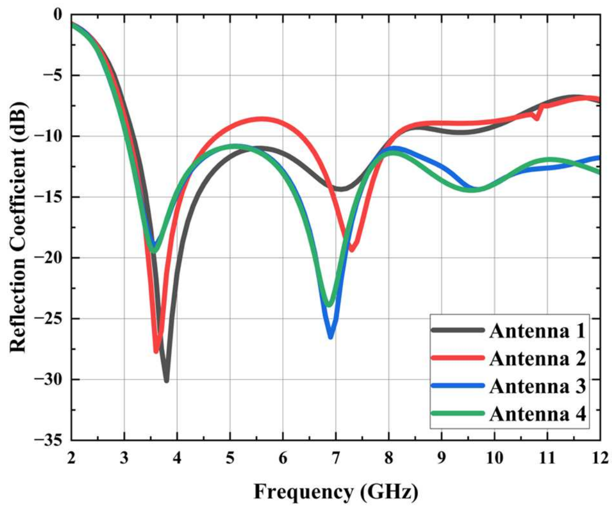


Fig. 5. The $S_{11}$ plot for composed fractal iterations.

### *B. Effect of fractal generations*

The simulated and observed fractal iterations shown in Fig. 2 are carried out for increased IBW. According to Fig. 5, the designed antenna has a broad 9 GHz bandwidth with an $S_{11}$ of less than 10 dB from 3 to 12 GHz. Studies show that the self-similar characteristics and increased electrical length based on fractal generations offer the radiator-wide IBW.

### *C. Effect of Ground Length $L_e$*

The partial ground length is denoted by the parameter $L_e$, as depicted in Fig. 3(c). Fig. 6 illustrates the impact of various $L_e$ values. The IBW at $S_{11}$ is obtained with several resonances at less than -10 dB when the length is decreased. Reducing the length '$L_e$' will result in a lower return loss at higher resonant frequencies.

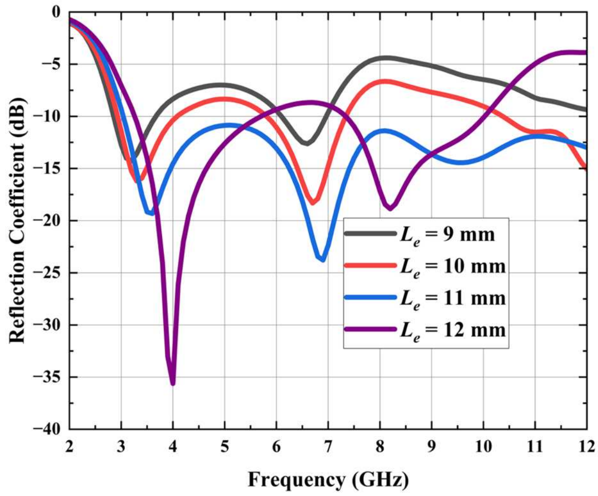


Fig. 6. The $S_{11}$ plot for different values of ground length $L_e$.

### *D. Effect of Rectangular Slit in the Ground Plane*

In Fig. 7, the addition of a rectangular slit on the ground plane directly below the feed is displayed and contrasted for various values of $L_p$. An impedance match can be attained by the addition of a rectangular slit, which causes coupling between the radiating element and the ground. The performances demonstrate that the return loss for $L_p$ = 3.5 mm is acceptable in comparison to other $L_p$ values, which is caused by improved impedance matching.

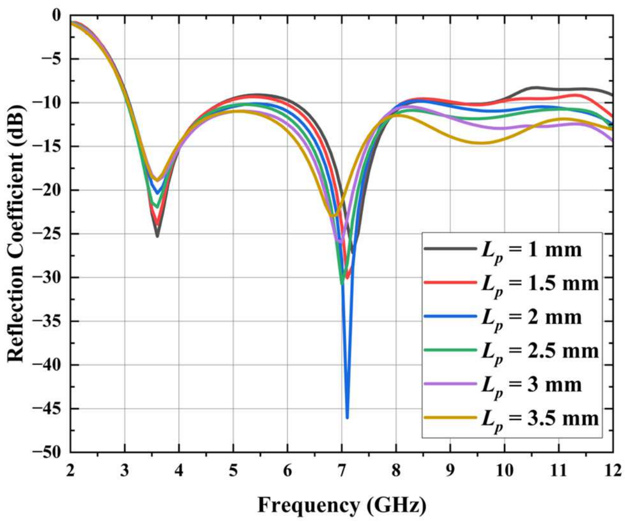


Fig. 7. The $S_{11}$ plot for different slit lengths $L_p$.

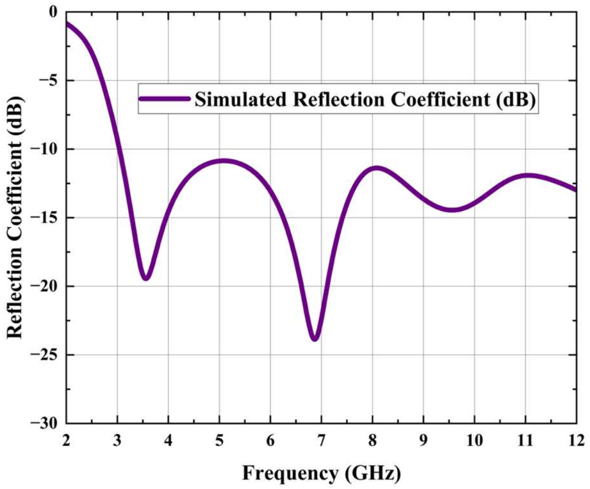


Fig. 8. A simulated $S_{11}$ plot of the design.

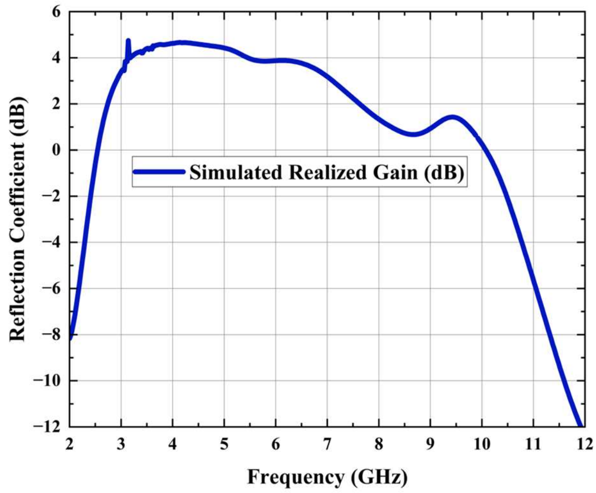


Fig. 9. A simulated realized gain plot.

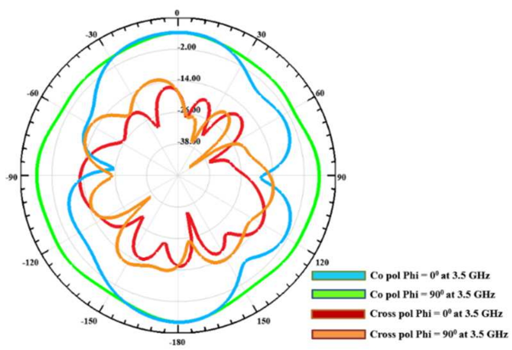


(a)

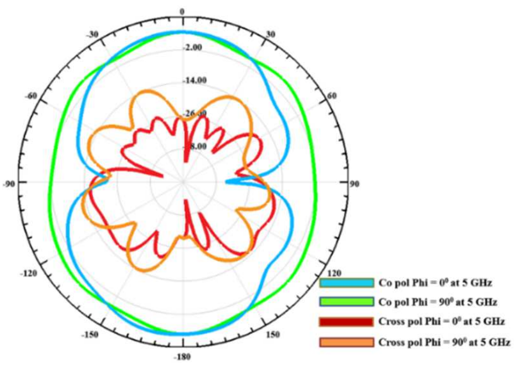


(b)

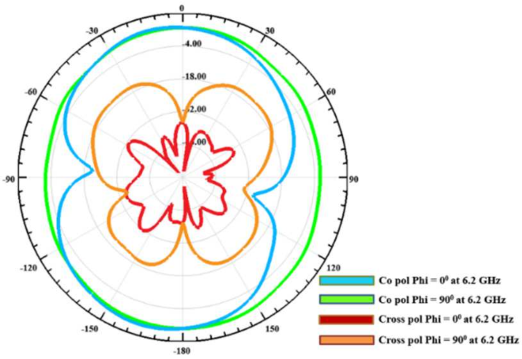


(c)

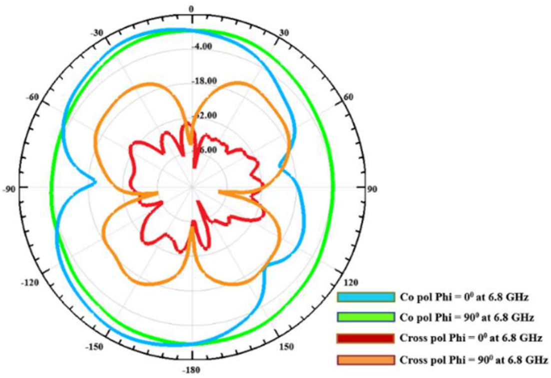


(d)

Fig. 10. The radiation patterns at (a) 3.5 GHz, (b) 5 GHz, (c) 6.2 GHz, and (d) 6.8 GHz.

### *E. Simulated Reflection Coefficient, Gain, and Radiation Pattern*

The reflection coefficient plot is shown in Fig. 8. The fractal structure's operating frequency range is from 3 GHz to 12 GHz. Fig. 9 shows the realized gain plot of the designed structure. It has a peak realized gain response of 4.7 dBi at 4.1 GHz with an omnidirectional radiation pattern covering the operational band. Increased losses, the formation of higher-order modes, and a larger XPD component are the reasons for the variation in realized gain at higher frequencies. The simulated radiation patterns are displayed in Fig. 10(a)-(d) from the lowest frequency of 3.5 GHz to the highest frequency of 6.8 GHz. The XPD reduces in the E or YZ-plane from lowest to highest resonances and increases in the H or XZ-plane because cross-field components occur in the bottom half of the radiating element and feed line. The patterns clearly show that the design structure generates cross-polarization fields of 40 dB with maximum radiation at resonance frequencies of 3.5 GHz, 5 GHz, 6.8 GHz, and 9.5 GHz.

## IV. Performance Comparison

Results for the designed radiator, including IBW, overall dimension, and gain variations, are compiled. The designed structure is distinguished because it is compact in dimensions, has a substrate thickness of 1 mm, and has an IBW of 120% across the whole IBW compared to other structures. Table II shows that the proposed fractal radiator has a high gain, small dimension, and better IBW performance, making it suitable for UWB (3.1 GHz – 10.6 GHz) wireless communication services.

**TABLE II**
Comparison of Recently Developed Fractal Antennas with the Proposed Design

| Ref. No. | Dimension ($mm^3$) | Shape of Patch | Fractal Geometry | No. of Iterations | Substrate Material | Peak Gain (dBi) | Frequency Band (GHz) | Applications |
|---|---|---|---|---|---|---|---|---|
| [5] | 30 × 30 × 1.5 | Square | Square | 3 | Rogers TMM 4 | 4.22 | 2.97 – 5.77 | Wireless application |
| [6] | 70 × 40 × 1.6 | Square | Star | 3 | FR-4 | 3.5 | 1.87 – 4.78 | Wideband application |
| [15] | 30 × 30 × 1.6 | Circular | Square, Circular | 3 | FR-4 | 3 | 3 – 12 | UWB application |
| [16] | 38.2 × 28 × 0.8 | Rectangular | Koch curve | 2 | Jeans substrate | 4.12 | 0.72, 3.89, 5.45 | Wireless applications |
| [17] | 24 × 35 × 1.3 | Hexagonal | Sierpinski | 2 | FR-4 | ~4 | 2.7 – 11.2 | UWB application |
| Proposed work | 30 × 30 × 1 | Pentagonal | Koch curve | 2 | Roger RT/Duroid 5880 | 4.7 | 3 – 12 | UWB application |

## V. CONCLUSION

A miniaturized linearly polarized fractal antenna is proposed for UWB applications. The Koch fractal geometry with microstrip feedline is used to design the antenna. A partial ground technique with a rectangular-shaped slit is also applied to obtain a wideband. The offered bandwidth of the proposed antenna is capable of covering 3 GHz - 12 GHz. The proposed fractal antenna provides a better radiation pattern and wide operating bandwidth of 9 GHz with multiple resonances, and correspondingly, the peak gain is 4.7 dBi at 4.1 GHz resonant frequencies. The designed radiator is reasonably good for wireless communication systems and can be suitable for UWB wireless communication services.

## REFERENCES


[1] H. Douglas and R. Mittra, *Frontiers in electromagnetics*, vol. 2, 2000.

[2] C. A. Balanis, *Antenna theory: analysis and design*, John wiley & sons, 2016.

[3] A. T. Abed, "A Novel Coplanar Antenna Butterfly Structure for Portable Communication Devices: A Compact Antenna With Multioperating Bands," *IEEE Antennas and Propagation Magazine*, vol. 62, no. 3, pp. 83-89, June 2020.

[4] N. K. Darimireddy, R. R. Reddy and A. M. Prasad, "A Miniaturized Hexagonal-Triangular Fractal Antenna for Wide-Band Applications [Antenna Applications Corner]," *IEEE Antennas and Propagation Magazine*, vol. 60, no. 2, pp. 104-110, April 2018.

[5] S. N. R. Rizvi *et al*., "Wideband Small Fractal Antenna with Simple Design Strategy for 5G Sub-6-GHz Wireless Communications," *2021 XXXIVth General Assembly and Scientific Symposium of the International Union of Radio Science (URSI GASS)*, Rome, Italy, pp. 1-4, 2021.

[6] S. Pandav, T. K. Das, K. R. Samyuktha, S. K. Behera, G. Sadhukhan and M. Mohanty, "Design of Star-Shaped Fractal Antenna for Wideband Applications," *2020 IEEE International Students' Conference on Electrical,Electronics and Computer Science (SCEECS)*, Bhopal, India, pp. 1-4, 2020.

[7] T. K. Das, D. Prasad Mishra, S. Pandav and S. K. Behera, "Design of a Wideband Pythagorean-tree shaped Fractal Monopole Antenna for RFID Applications," *2019 IEEE Indian Conference on Antennas and Propogation (InCAP)*, Ahmedabad, India, pp. 1-4, 2019.

[8] Y. B. Chaouche, M. Nedil, B. Hammache and M. Belazzoug, "Design of Modified Sierpinski Gasket Fractal Antenna for Tri-band Applications," *2019 IEEE International Symposium on Antennas and Propagation and USNC-URSI Radio Science Meeting*, Atlanta, GA, USA, pp. 889-890, 2019.

[9] W. Kuhirun, W. Silabut, V. Kesornpatumanun and P. Boonek, "Design of a dual-band patch antenna with Peano-Gosper fractal slot," *2016 IEEE 5th Asia-Pacific Conference on Antennas and Propagation (APCAP)*, Kaohsiung, Taiwan, pp. 291-292, 2016.

[10] Pandav, S., Sadhukhan, G., Das, T.K. *et al.,* "Circularly polarized high gain Koch fractal antenna for space applications," *Sādhanā,* vol. **47**, no. 276, 2022.

[11] A. Arif, M. Zubair, M. Ali, M. U. Khan and M. Q. Mehmood, "A Compact, Low-Profile Fractal Antenna for Wearable On-Body WBAN Applications," *IEEE Antennas and Wireless Propagation Letters*, vol. 18, no. 5, pp. 981-985, May 2019.

[12] Y. K. Choukiker, S. K. Sharma and S. K. Behera, "Hybrid Fractal Shape Planar Monopole Antenna Covering Multiband Wireless Communications with MIMO Implementation for Handheld Mobile Devices," *IEEE Transactions on Antennas and Propagation*, vol. 62, no. 3, pp. 1483-1488, March 2014.

[13] J. Tian *et al*., "Design of a Flexible UHF Hilbert Antenna for Partial Discharge Detection in Gas-Insulated Switchgear," *IEEE Antennas and Wireless Propagation Letters*, vol. 22, no. 4, pp. 794-798, April 2023.

[14] S. Bhaskar, M. G. Siddiqui, S. Singhal and A. Bansal, "Miniaturized Circularly Polarized Vicsekcross-Shaped Slot Antenna for UHF-RFID Reader Handset Applications," *IEEE Journal of Radio Frequency Identification*, vol. 6, pp. 515-523, 2022.

[15] M. Jayaram, K. N. Devnesh and B. M. Anjaneyulu, "Design of a UWB Antenna Utilising Fractal Geometry and EBG Structures for Wireless Applications," *2023 International Conference on Intelligent Systems for Communication, IoT and Security (ICISCoIS)*, Coimbatore, India, pp. 185-189, 2023.

[16] R. Deshpande, V. R. Tottempudi and R. S. R. B, "Koch Fractal Iterations Based T-Patch Antenna for Low Giga Hertz and Wireless Applications," *2022 IEEE International RF and Microwave Conference (RFM)*, Kuala Lumpur, Malaysia, pp. 1-4, 2022.

[17] H. Yuan, F. -S. Zhang and Y. -F. Liu, "A Compact Ultra-Wideband Fractal Antenna with Dual Band-Notched Characteristics," *2021 International Conference on Microwave and Millimeter Wave Technology (ICMMT)*, Nanjing, China, pp. 1-3, 2021.

[18] N. Rao, "Modified Sierpinski and its use in Fractal Patch Antenna for Miniaturization and Multiband Behavior," *2022 IEEE Microwaves, Antennas, and Propagation Conference (MAPCON)*, Bangalore, India, pp. 1804-1809, 2022.

[19] K. Patel, S. Pandav and S. K. Behera, "Compact Hexagonal Monopole Antenna using Defected Ground Structure (DGS) for S and C-Band Applications," *2022 International Conference on Futuristic Technologies (INCOFT)*, Belgaum, India, pp. 1-4, 2022.

[20] K. Patel and S. K. Behera, "A Miniaturized Wideband Fractal Antenna Combining Sierpinski and Minkowski Fractals," *2023 3rd International Conference on Range Technology (ICORT)*, Chandipur, Balasore, India, pp. 1-4, 2023.